International Journal for Research in Engineering Application & Management (IJREAM)
ISSN : 2454-9150 Vol-06, Issue-07, OCT 2020

Nickel oxide thin films formed by DC magnetron sputtering: Influence of oxygen partial pressure on the physical properties

K. Ravindra, M. Hari Prasad Reddy and S. Uthanna*

Department of Physics, Sri Venkateswara University, Tirupati, India. *uthanna.suda@gmail.com

Abstract - Thin films of nickel oxide were prepared on glass and p- silicon substrates by direct current magnetron sputtering of metallic nickel target at oxygen partial pressures (pO_2) in the range $8x10^{-5}$ - $6x10^{-4}$ mbar. The deposited films were characterized for the composition, chemical binding configuration, structure, electrical and optical properties. The influence of oxygen partial pressure on the physical properties was studied. XPS studies indicated the growth of films with Ni^{2+} oxidation state of NiO. The films deposited at $\geq 4x10^{-4}$ mbar were of stiochiometric NiO with polycrystalline with crystallite size of 16.2 nm. FTIR spectra showed the characteristic vibrational mode of NiO. The films formed at oxygen partial pressures < $4x10^{-4}$ mbar were of nickel and NiO with amorphous nature. The electrical resistivity increased, and the hole mobility decreased with increase of oxygen partial pressure. The optical band gap increased from 3.02 eV to 3.70 eV with increase of oxygen partial pressure.

Keywords – pO_2 , NiO, Ni^{2+}, FTIR.

I. INTRODUCTION

Transition metal oxides attracted much attention because of their diverse physical properties for applications in microelectronics and optoelectronic devices [1]. These are semiconductors or metallic oxides namely zinc oxide, titanium oxide, nickel oxide, ferrous oxide and chromium oxide. Among these oxides, nickel oxide (NiO) received much interest due to its low cost, chemically stable with good electrical, optical and magnetic properties made potential for device applications. NiO is a stable compound with wide band gap of ~ 3.7 eV and find application in electrochromic devices [2],[3] hole injection layer in optoelectronic devices [4],[5],[6] charge trapping layer in memory devices [7], anode buffer layer in organic solar cells [8] and sensing of carbon monoxide and hydrogen gases [9],[10]. NiO thin films can be produced various chemical routes namely chemical bath deposition [11], spray pyrolysis [12], and physical methods such as vacuum evaporation [13], electron beam deposition [2],[14] pulsed laser deposition [6], DC magnetron [15],[16] and RF magnetron [17],[18],[19] sputtering. Among these thin film deposition methods, DC reactive magnetron sputtering considered to be the industrially practiced technique for production of metal oxide films on large area substrates by sputtering of metallic target in the presence of reactive gas of oxygen. The physical properties of the deposited films critically depend on the sputter parameters namely the oxygen partial pressure, substrate temperature, sputter power and bias voltage applied to the substrate. In the present study, we deposited NiO thin films by DC reactive magnetron sputtering of metallic nickel target at different oxygen partial pressures. The influence of oxygen partial pressure on the chemical composition, core level binding energies, structure and surface morphology, and electrical and optical properties of NiO films was systematically studied.

II. EXPERIMENTATION

NiO thin films were deposited onto glass and p-type silicon substrates using DC reactive magnetron sputtering technique. Hind Hivac box type coating system pumped by diffusion pump backed by rotary pump was employed to create ultimate pressure of $5x10^{-6}$ mbar. Oxygen and argon were used as reactive and sputter gases for deposition of the films. After achieving the ultimate pressure in the sputter chamber, oxygen gas was admitted into the sputter chamber through fine controlled needle valve to achieve the oxygen partial pressure in the range $8x10^{-5}$ - $6x10^{-4}$ mbar. Then argon gas was introduced to obtain the sputter chamber to reach the sputter pressure of $3x10^{-2}$ mbar. Metallic target of nickel (99.99% pure) of 50 mm diameter and 3 mm thick was used for deposition of films on the unheated substrates. DC variable power supply (0 – 1000 V and 50 – 1000 mA) was used for deposition of the films at sputter power of 90 W. Deposition parameters maintained for the growth of the films are given in the table 1. In order to deposit the films with almost equal thickness, the deposition time was varied depending on the oxygen partial pressure maintained during the growth of the films. Thickness of the deposited films measured with

 DOI : 10.35291/2454-9150.2020.0656 © 2020, IJREAM All Rights Reserved.

ISSN : 2454-9150 Vol-06, Issue-07, OCT 2020

Table 1. Parameters maintained for deposition of nickel oxide thin films

Deposition method	: DC magnetron sputtering
Sputter target	: Nickel
Target - substrate distance	: 50 mm
Substrates	: Glass and p- silicon
Substrate temperature	: 30°C
Sputter power	: 90 Watt
Ultimate pressure	: $5x10^{-6}$ mbar
Oxygen partial pressure (pO_2)	: $8x10^{-5}$- $6x10^{-4}$ mbar
Sputter pressure	: $3x10^{-2}$ mbar

Dektak depth profilometer and was in the range 110 - 130 nm. The deposited films were characterized for chemical composition, structure, electrical and optical properties. Chemical composition of the films was analyzed with energy dispersive X-ray analyzer (Oxford Instruments Inca Penta FETX3) attached to the scanning electron microscope (Carl Zeiss model EVO MAIS). Crystallographic structure, crystallite size, dislocation density and stain developed in the films was studied with X- ray diffractometer (X'pert Pro PAN Analytical) with copper (Cu K_α) radiation with wavelength of 0.15406 nm. Surface morphology of the deposited films was analyzed with atomic force microscope (Sicko Instruments Inc. SII) equipments with SPA400 cantilever operated in dynamic force mode. Electrical resistivity of the deposited films was measured using van der Pauw method. Optical transmittance of the films formed on glass substrates was recorded with JASCO (model V570) UV-Vis-NIR double beam spectrophotometer in the wavelength range 300 - 1000 nm to understand the optical absorption and to determine the optical band gap of the films.

III. RESULTS AND DISCUSSION

Deposition rate of the nickel oxide films depend on the oxygen partial pressure prevailed in the sputter chamber. Variation of deposition rate of the films on oxygen partial pressure is shown in figure 1. The deposition rate of the films formed at low oxygen partial pressure of $8x10^{-5}$ mbar was 13.4 nm/min. As the oxygen pressure increased to $6x10^{-4}$ mbar, the deposited rate decreased to 7.2 nm/min. High deposition rate at low oxygen partial pressures was due high sputter yield of metallic species. As the oxygen partial pressure increased the oxidation of sputter target takes places. The sputter yield of oxide is less than the metal hence the deposition rate decreased. It is in accordance with the achieved results in DC magnetron sputtered ZnO films [18].

Chemical composition

Figure 2 shows the energy dispersive X-ray analysis spectra of nickel oxide films formed on silicon substrates at different oxygen partial pressures. The spectra of the films showed the characteristic kinetic energy peaks of nickel and oxygen along with silicon. Silicon in the spectrum present was due to the signal from silicon substrate. EDAX spectra showed the intensity of oxygen peak enhanced with the increase of oxygen partial pressure. Chemical composition of the films was evaluated from the intensity of the kinetic energy peaks of the films formed at different oxygen partial pressures are given in table 2. The films

Table 2. Chemical composition of NiO_2 films determined with from EDAX

Oxygen partial pressure (pO_2)	Chemical composition (at. %)	
	Nickel (at. %)	Oxygen (at. %)
$8x10^{-5}$ mbar	59.4	40.6
$2x10^{-4}$ mbar	53.1	46.9
$4x10^{-4}$ mbar	49.2	50.8

deposited at low oxygen partial pressure of $8x10^{-5}$ mbar contained the content of nickel 59.4 at. % and oxygen 40.6 at. %. The films deposited at $4x10^{-4}$ mbar were with nickel 49.2 at. % and oxygen 50.8 at.%. Low content of oxygen in the films formed at low oxygen partial pressures was due to deficiency of oxygen in the sputter chamber form nickel oxide. Hence the films were of nickel oxide along with nickel. As the oxygen partial pressure increased to $4x10^{-4}$ mbar the sputtered species effectively react with available oxygen and form stoichiometric NiO.

X-ray photoelectron spectroscopic studies

The core level binding energies and chemical states of the constituent atoms or molecules of the films was studied with X-ray photoelectron scope. Figure 3 shows the survey scan spectra of NiO films deposited at different oxygen partial pressures. The spectra consists the core level binding energy peaks of nickel and oxygen. The core level binding energies observed at about 66.63 eV and 114.10 eV were related to nickel Ni 3p and Ni 3s, 284 eV correspond to carbon C 1s, 530 eV connected to oxygen O 1s, 855 eV and 870 eV of Ni $2p_{3/2}$ and Ni $2p_{1/2}$ and 975.81 eV of Ni 2s. The carbon present in the films was due to the exposure of film to the atmosphere before the XPS analysis. In order to eliminate the surface carbon, the films were sputtered with argon ions for two minutes. Figure 3 shows the narrow scan spectra of (b) nickel Ni 2p and (c) oxygen O 1s of NiO films formed at different oxygen partial pressures. The core level binding energies were located at 853.05 eV and 855.05 eV related to Ni $2p_{3/2}$, and 872.39 eV and 878.87 eV correspond to Ni $2p_{1/2}$. The films deposited at low oxygen partial pressure of $8x10^{-5}$ mbar showed the core level binding energies at 853.09 eV and 872.39 eV related to Ni^0 oxidation state and 855.05 eV and 878.87 eV for Ni^{2+} oxidation state NiO [20] revealed the growth of mixed phase nickel and NiO films. It is to be noted that the binding energies of 852.6 eV, 854.6 eV and 856.1 eV related to Ni $2p_{3/2}$ of Ni^0, Ni^{2+} and Ni^{3+} oxidation states of

 DOI : 10.35291/2454-9150.2020.0656 © 2020, IJREAM All Rights Reserved.

Ni, NiO and Ni_2O_3 [21]. In the case of the films deposited at oxygen partial pressure of 2x10^{-4} mbar the binding energies shifted towards higher energy side. The films formed at 4x10^{-4} mbar consist of 855.4 eV of NiO. In the case of oxygen O 1s, the films formed at 8x10^{-5} mbar exhibited the binding energies at 528.36 eV and 530.4 eV related to the Ni and NiO and those deposited at 4x10^{-4} mbar showed the binding energy at 530.51 eV of single phase NiO [2]. Yun et al. [19] noticed the core level binding energies of O 1s at 529.2 eV in RF sputtered NiO films. The shakeup peaks were also seen in all the films. These studies revealed that the films formed at oxygen partial pressure of 4x10^{-4} mbar were of single phase NiO.

Structural studies

Figure 4 shows XRD profiles of nickel oxide films formed at different oxygen partial pressures. It is seen that the films formed at low oxygen partial pressure of 8x10^{-5}mbar consist of weak diffraction reflections at 2θ = 37.12°, 43.21° and 62.67° in the amorphous background. At oxygen partial pressure 2x10^{-4} mbar the films showed the diffraction peaks at 2θ = 37.09°, 43.10° and 62.59° related to the (111), (200) and (220) reflection of with face centred cubic NiO (JCPDS Card No. 89-7130).The films formed at 4x10^{-4} mbar showed that the intensity of the reflections increased due to improvement in the crystallinity. Further (111) reflection was more intense than those deposited at low oxygen partial pressures. Crystallite size of the films was determined from the (111) peak of NiO using Debye-Scherrer's equation [22]

$$D = k\lambda/\beta\cos\theta \qquad \text{------ (1)}$$

Where θ is the diffraction angle, λ the copper X-raywavelength (0.15406 nm), β the full width at half maximum intensity of diffraction peak and k the correction factor for copper Kα radiation (k = 0.9). Crystallite size of the films determined from the (111) reflection increased from 6.2 nm to 16.8 nm with increase of oxygen partial pressure from 2x10^{-4} mbar to 4x10^{-4} mbar. Dislocation density (δ) and strain (ε)developed in the films were calculated from the X-ray diffraction peak of (200) of NiO employing the relations,

$$\delta = 1/D^2 \qquad \text{----- (2)}$$

And $$\varepsilon = \beta\cos\theta/4 \qquad \text{------ (3)}$$

The dislocation density decreased from 2.6 x10^{16} lines/m^{-2} to 0.3x10^{16} lines/m^{-2} and the strain decreased from 5.45x10^{-3} to 2.06x10^{-3} with increase of oxygen partial pressure from 2x10^{-4} mbar to 4x10^{-4} mbar.

Fourier transform infrared studies

The NiO films deposited on p- silicon was used for Fourier transform infrared spectroscopic studies. Fourier transform infrared transmittance spectra of the films formed at different oxygen partial pressures are shown in figure 5. The films formed at oxygen partial pressure of 8x10^{-5} mbar not shown any absorption bands due to amorphous nature. The films deposited at oxygen partial pressures ≥ 4x10^{-4} mbar were of polycrystalline contained the bands at 409 cm^{-1}, 751 cm^{-1} and 895 cm^{-1}. Absorption band located at 407 cm^{-1} was the stretching vibration mode of Ni – O [23], and the bands located at 751 cm^{-1} and 895 cm^{-1} were the bending vibration modes of O – Ni – O [24],[25]. It is in accordance with the reported infrared vibrational modes in spray deposited NiO films [12].

Surface morphology

Atomic force microscopic studies were performed on the films formed at different oxygen partial pressures. Atomic force micrographs of the films formed at different oxygen partial pressures are shown in figure 6. Grown grains were of spherical shape with uniform distribution on the surface of the films. Size of the grains increased from 95 nm to 119 nm with increase of oxygen partial pressure from 8x10^{-5} mbar to 4x10^{-4} mbar respectively. The root mean square roughness of the films increased from 3.7 nm to 5.0 nm with increase of oxygen partial pressure.

Electrical properties

Figure 7 shows the electrical resistivity of NiO films deposited at various oxygen partial pressures. At low oxygen partial pressure of 8x10^{-5} mbar the resistivity of the films was 0.5 Ωcm. The films formed at oxygen partial pressure of 6x10^{-4} mbar showed the resistivity of the film increased to 10.2 Ωcm. Low electrical resistivity at low oxygen partial pressures was due to the presence of oxygen ion vacancies. At higher oxygen pressures the oxygen ion vacancies decreased and form NiO hence increase in the resistivity of the films. Such an increase in the resistivity increased from 8x10^{-3} Ωcm to 2 Ωcm with increase of oxygen partial pressure from 1.3 mbar to 13 mbar in DC magnetron sputtered films [15]. Zhao et al. [17] noticed that the resistivity from 9x10^{-2} Ωcm to 4 Ωcm with increase of oxygen flow rate of 20% to 80% in RF magnetron sputtered films. Hall mobility measurements indicated that the deposited films were of p- type in electrical conduction. The hole mobility of the films decreased 5.4 cm^2/V.sec to 1.9 cm^2/V.sec and hole concentration decreased from 2.3x10^{18} cm^{-3} to 3.2x$10^{17}$$cm^{-3}$ with increase of oxygen partial pressure from 8x10^{-5} mbar to 6x10^{-4} mbar respectively.

Optical properties

Optical transmittance of the films formed on glass substrates was studied to determine the optical band gap. The optical transmittance of the films was influenced by the oxygen partial pressure maintained during the deposition of the films. Optical transmittance spectra of NiO films formed at different oxygen partial pressures shown in figure 8. Transmittance of the films deposited at low oxygen partial pressure of 8x10^{-5} mbar was 36%. As the oxygen partial pressure increased to 6x10^{-4} mbar the transmittance

 DOI : 10.35291/2454-9150.2020.0656 © 2020, IJREAM All Rights Reserved.

enhanced 55%. At low oxygen partial pressures, the low transmittance was due to scattering of photons by the oxygen ion vacancies that is metallic nickel. When oxygen partial pressure increased to $4x10^{-4}$ mbar the oxygen ion vacancies reduced hence increase in the transmittance of the films. The fundamental optical absorption edge of the films shifted towards blue side with increase of oxygen partial pressure. The optical absorption coefficient (α) was determine from the optical transmittance (T) and thickness of the films (t) using the relation

$$A=-(1/t)\ln(T) \quad - (4)$$

The optical band gap (E_g) of the films was determined by fitting the absorption coefficient to the Tauc's relation [26]

$$(\alpha h\nu)^2 = A(h\nu- E_g)^{1/2} \quad ----- (5)$$

where A is the edge width parameter. Plots of $(\alpha h\nu)^2$ versus photon energy of the films formed at different oxygen partial pressures are shown in figure 9. Optical band gap of the films formed at low oxygen partial of $8x10^{-5}$ mbar was 3.02 eV. As the oxygen partial pressure increased to $6x10^{-4}$ mbar the band gap increased to 3.70 eV. Low band gap at low oxygen pressures was due to nonstoichiometric films that is NiO along with Ni. The optical band gap of the NiO films deposited at oxygen partial pressure at $4x10^{-4}$ mbar was 3.66 eV. Zhao et al. [17] noticed that the band gap increased from 3.25 eV to 3.80 eV with increase of oxygen from 20% to 80% in RF magnetron sputtered films, and 3.70 eV in electron beam evaporated [3] and 3.61 eV in DC magnetron sputtered [4] films.

IV. CONCLUSIONS

Nickel oxide thin films were deposited on glass and p- Si substrates DC magnetron sputter deposition at different oxygen partial pressures in the range $8x10^{-5}$ - $6x10^{-4}$ mbar. The deposited films were characterized for the chemical composition, structure, electrical properties. The effect of oxygen partial pressure on the physical properties was investigated.

The NiO films formed at oxygen partial pressures < $4x10^{-4}$ mbar were of NiO along with nickel and those formed at ≥ $4x10^{-4}$ mbar were of NiO. XPS analysis of the films formed at $4x10^{-4}$ mbar showed the core level binding energies related Ni^{2+} oxidation state confirm the growth of NiO. FTIR studies also confirmed the existence of characteristic vibration modes of Ni – O and O – Ni – O characteristics of NiO.

The films formed at $8x10^{-5}$ mbar were of amorphous in nature while those deposited at oxygen partial pressure ≥ $4x10^{-4}$ mbar were polycrystalline with cubic structure NiO. The crystallite size increased from 6.2 nm to 16.8 nm with increase of oxygen partial pressure from $2x10^{-4}$ mbar to $4x10^{-4}$ mbar.

Electrical resistivity of the increased from 0.5 Ωcm to 10.2 Ωcm and hole mobility decreased from 5.4 to 1.9 cm^2/V.sec with increase of oxygen partial pressure. Optical band gap of the films increased from 3.02 eV to 3.70 eV with increase of oxygen partial pressure from $8x10^{-5}$ to $6x10^{-4}$ mbar.

In conclusion, polycrystalline with cubic structured NiO thin films deposited at the optimised oxygen partial pressure of $4x10^{-4}$ mbar with electrical resistivity of 7.2 Ωcm, hole mobility of 2.2 cm^2/V.sec and optical band gap of 3.66 eV.

ACKNOWLEDGEMENT

Mr. K. Ravindra is thankful to the University Grants Commission (UGC), New Delhi for award of Senior Research Fellowship under UGC-BSR-RFSMS Fellowship Program. Prof. S. Uthanna is thankful to the UGC, New Delhi India for the award of UGC-BSR Faculty Fellowship.

REFERENCES

[1] A.A. Demkov, P. Panath, K. Fredrickson, Integrated films of transition metal oxides for information technology, Microelectron. Eng., vol. 147, pp 285-289, 2015.

[2] Q. Liu, Q. Chen, Q. Zhang, Y. Xiao, X. Zhang, G. Dong, M.P.D. Ogletree, H. Terryn, K. Baert, F. Reniers and X. Diao, In-situ electrochromic efficiency of nickel oxide thin films: Origin of electrochemical process and electrochromic degradation, J. Name, 2017, doi:10.1039/C7TC04696K.

[3] T. Abzieher, S. Moghadamzadeh, F. Schackmar, H. Feggers, F. Sutterluti, A. Farooq, D. Kojda, K. Habicht, R. Schmager, A. Mertins, R. Azmi, L. Klocht, J.A. Schwenzer, M. Hatterich, U. Lemmer, B.S. Richards, M. Pawalla and U.W. Paetzold, Electron beam evaporated nickel oxide hole transport layer for perovskite based photovoltaics, Adv. Energy Mater., 1802995, 2019.

[4] Y. Zhang, Thermal oxidation fabrication of NiO films for optoelectronic devices, Appl.Surf. Sci., vol. 344, pp 33-37, 2015.

[5] J.H. Tsai, S.M. Hsu, I.C. Chens, C.C. Hsu, J.Z. Chen, Conversion of dense and continuous NiO compound thin films using nitrogen DC pulsed atmospheric pressure plasma jet, Ceram. Int., vol. V45, pp 22078-84, 2020.

[6] Z. Zhao, A.H. Baillie and S.P. Bremne, Pulsed laser deposited nitrogen oxide on silicon as hole selection contacts, J. Vac. Sci. Technol. B, vol, 38, pp 014013, 2020.

[7] M.L. Lee, H. Chen, C.H. Kao, R.K. Mahanty, W.K. Sun, C.F. Lin, C.Y. Lin and K.M. Chang, Physical and electrical properties of flash memory devices with NiO_2 charge trapped layer, Vacuum, vol. 140, pp 47-52, 2017.

[8] S.Y. Park, H.R. Kim, Y.J. Kang, D.H. Kim. J.W. Kang, Organic solar cells employed nitrogen oxide thin films as the anode buffer layer, Solar Energy Mater. Solar Cells, vol. 94, pp 2332-2338, 2010.

[9] A.A. Khaleed, A. Bello, J.K. Dangbenan, D.Y. Momodu, M.J. Medito and F.U. Ugbo, Effect of activated carbon on the enhancement of Co sensing performance of NiO, J. Alloy. Compd., vol. 694, 155-162, 2017.

[10] D. Abubakar, N.M. Ahmed, S. Mahmud and N. Algadri, Mater. Res. Exp., vol. 4, pp 075009, 2017.

[11] M.M. Gil, M.I.P. Monroy, M.C. Leal, D.C. German, A.G. Fontecha, M.A.Q. Lopez and M.S. Lerma, Mater, Sci. Semicond. Process., vol 72, 37-45, 2017.

[12] R. Barir, B. Benhaoua, S. Benhamida, A. Rahul, T. Sahraoui and R. Gheriani, Effect of precursor concentration on structure,

 DOI : 10.35291/2454-9150.2020.0656 © 2020, IJREAM All Rights Reserved.

ISSN : 2454-9150 Vol-06, Issue-07, OCT 2020

optical and electrical properties of NiO thin films prepared by spray pyrolysis, J. Nanomater., vol. 2017, pp 5204639, 2017.

[13] L. Raghavan, S. Ohja, I. Sulina, N.C. Mishra, K.M. Ranjith, M. Baenitz and D. Kanjilal, Thin Solid Films, vol 680, pp 40-46, 2019.

[14] D.R. Sahu, T.J. Wu, S.C. Wang, and J.L. Huang,Electrochromic behaviour of NiO film prepared by electron beam evaporation, J. Sci: Adv. Mater. Dev., vol. 2, pp 225-230, 2017.

[15] H. Sun, S.C. Chen, S.W. Hsu, C.K. Wen, T.H. Chuang and X. Wang, Structures, optical and electrical properties of NiO films by reactive magnetron sputtering at various working pressures of pure oxygen environment, Ceram. Int., vol. 43, pp S369-375, 2017.

[16] M. Wang, Y. Thimont, L. Presmane, X. Daio, A. Barnabe, The effect of the oxygen ratio control of DC reactive magnetron sputtering on as-deposited non-stoichiometric NiO thin films, Appl. Surf. Sci., vol. 419, pp 795-801, 2017.

[17] Y. Zhao, H. Wang, C. Wu, Z.F. Shi, F.B. Gao, W.C. Li, G.G. Wu, B.L. Zhang and G.T. Du, Structure, electrical and optical properties of NiO films by RF magnetron sputtering, Vacuum, vol. 103, pp 14-16, 2014.

[18] C. Li, T. Matsuda, T. Kawaharamura, H. Furuta, M. Furuta, T. Hiramatsu, T. Hirao, Y. Nakanishi and K. Ichinoiya, Comparision of structural and photoluminescence Properties of zinc oxide nanostructures influenced by gas ratio and substrate bias voltage during RFsputtering, J. Vac. Sci. Technol. B, vol. 29, pp C2B51, 2010.

[19] D.J. Yun and S.W. Rhee, Deposition of NiO_x thin films with RF magnetron sputtering and their characteristics as a source/drain electrode for the pentacene thin film transistor, J.Vac. Sci. Technol. B, vol. 26, pp 1787-1793, 2008.

[20] Y. Chen, Y. Sun, X. Dai, B. Zhang, Z. Ye, M. Wang and H. Wu, Tunable electrical properties of NiO thin films and p-type thin film transistors, Thin Solid Films, vol. 592, pp 195-199, 2015.

[21] A.F. Carley, S.D. Jackson, J.N. O'shea and M.W. Roberts, The formation and characterization of Ni^{3+} - An XPS investigations of potassium doped NiO, Surf. Sci., vol. 440, pp L868-L874, 2015.

[22] B.D. Cullity and S.R. Stock, Elements of X-ray Diffraction, Prentice Hall, Englewood Cliffs, NJ, pp 170, 2001.

[23] P.C. Yu, G. Nazri and C.M. Lampert, Spectroscopic and electrochemical studies of electrochromic hydrated nickel oxide films, Solar Energy Mater., vol. 16, pp 1-17, 1987.

[24] A.S. Adekudem J.A.O. Oyekunle and O.S. Oluwafemi, Comparative catalysis Properties of $Ni(OH)_2$ and NiO nanoparticles towards the degradation of nitrite (NO_2^-) and nitric oxide (NO), Int. J. Electrochem. Sci., vol. 9, pp 3008-3021, 2014.

[25] D.M. Fernandes, A.A.W. Hechenleitner and M.F. Silva, Preparation and Characterization of NiO, Fe_2O_3, $Ni_{0.04}Zn_{0.96}O$ and $Fe_{0.03}Ni_{0.97}O$ nanoparticles, Mater. Chem. Phys., vol.118, pp 447-452, 2009.

[26] J. Tauc, Amorphous and Liquid Semiconductors, Plenum Press, NY 2007.

Caption for figures

Figure 1 Variation of deposition rate of nickel oxide films with oxygen partial pressure.

Figure 2 EDAX spectra of nickel oxide films formed at different oxygen partial pressures.

Figure 3 XPS spectra of NiO films formed at different oxygen partial pressures: (a) survey scanand narrow scan of (b) nickel Ni 2p and (c) oxygen O 1s.

Figure 4 XRD profiles of nickel oxide films formed at different oxygen partial pressures.

Figure 5 FTIR transmittance spectra of NiO films formed at different oxygen partial pressures.

Figure 6 AFM micrographs of nickel oxide films formed at various oxygen partial pressures.

Figure 7 Electrical resistivity of NiO films deposited at various oxygen partial pressures.

Figure 8 Optical transmittance spectra of NiOfilms formed at different oxygen partial pressures.

Figure 9 Plots of $(\alpha h\nu)^2$ versus photon energy of NiO films formed at different oxygen partial pressures.

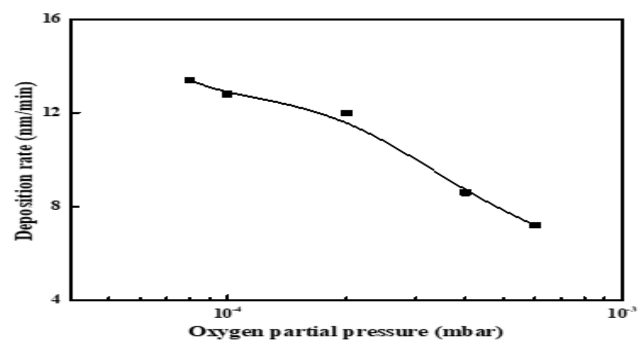

Figure 1 Variation of deposition rate of nickel oxide films with oxygen partial pressure.

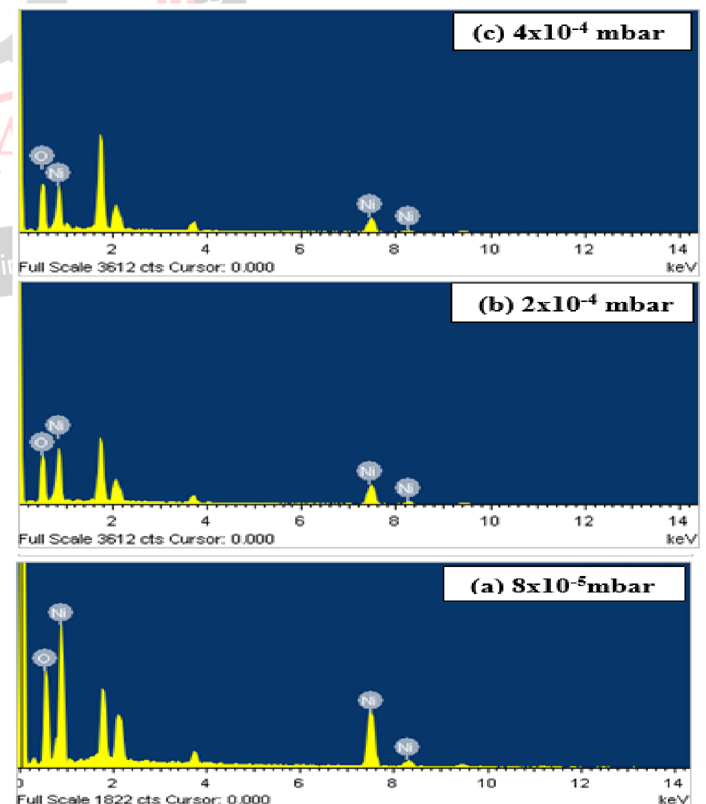

Figure 2 EDAX spectra of nickel oxide films formed at different oxygen partial pressures.

 DOI : 10.35291/2454-9150.2020.0656 © 2020, IJREAM All Rights Reserved.

ISSN : 2454-9150 Vol-06, Issue-07, OCT 2020

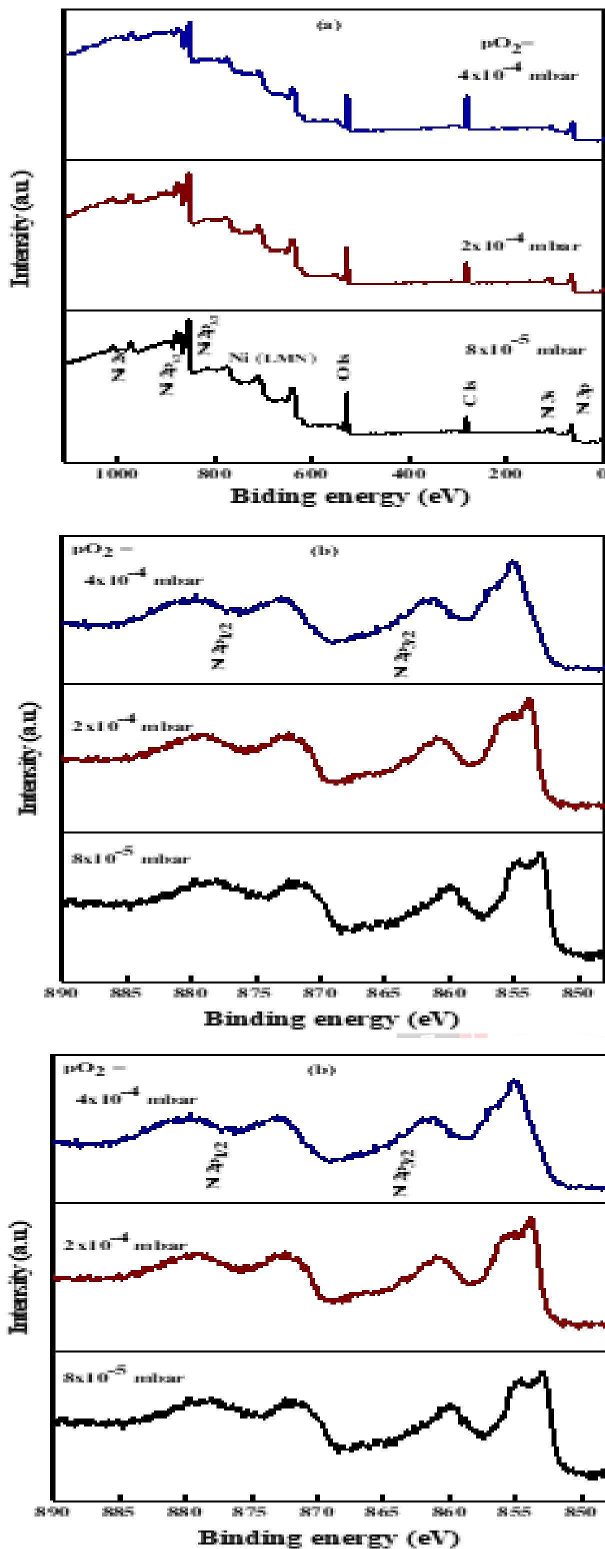

Figure 3 XPS spectra of NiO films formed at different oxygen partial pressures: (a) survey
Scan and narrow scan of (b) nickel Ni 2p and (c) oxygen O 1s.

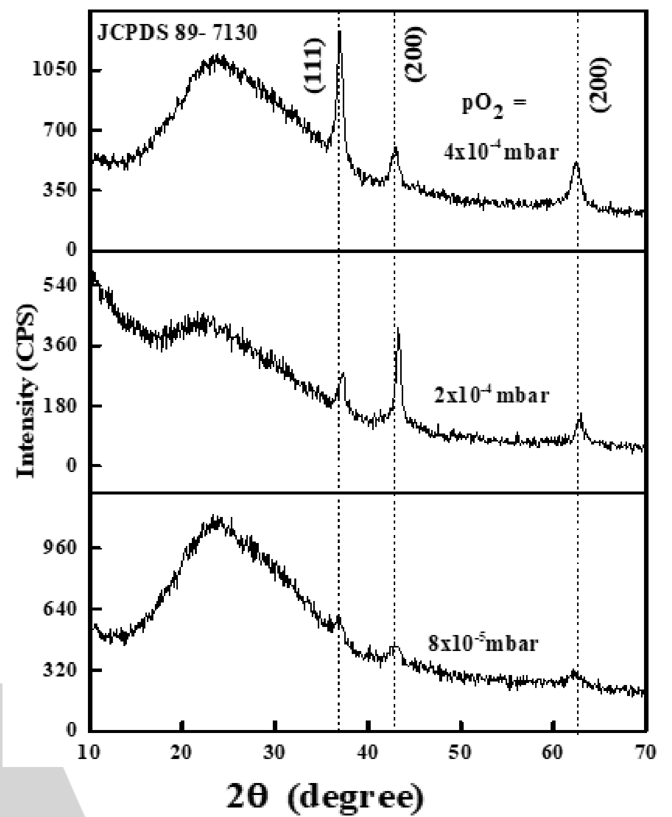

Figure 4 XRD profiles of nickel oxide films formed at different oxygen partial pressures.

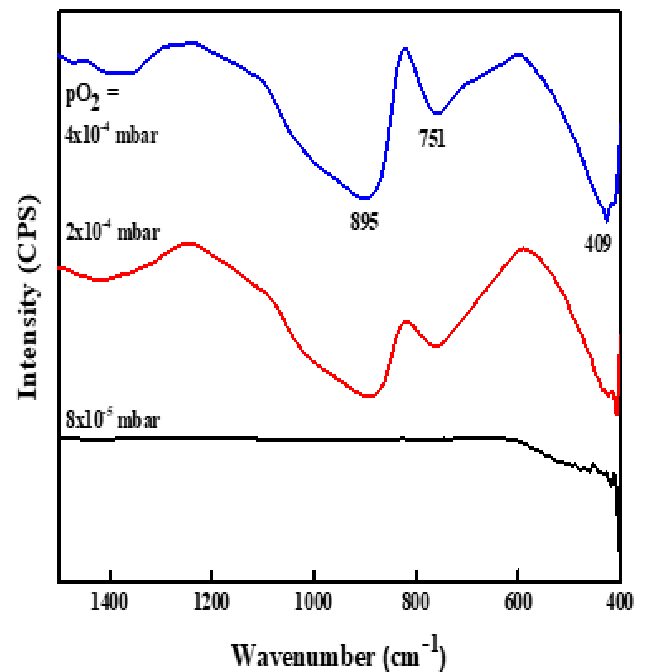

Figure 5 FTIR transmittance spectra of NiO films formed at different oxygen partial pressures.

DOI : 10.35291/2454-9150.2020.0656
© 2020, IJREAM All Rights Reserved.

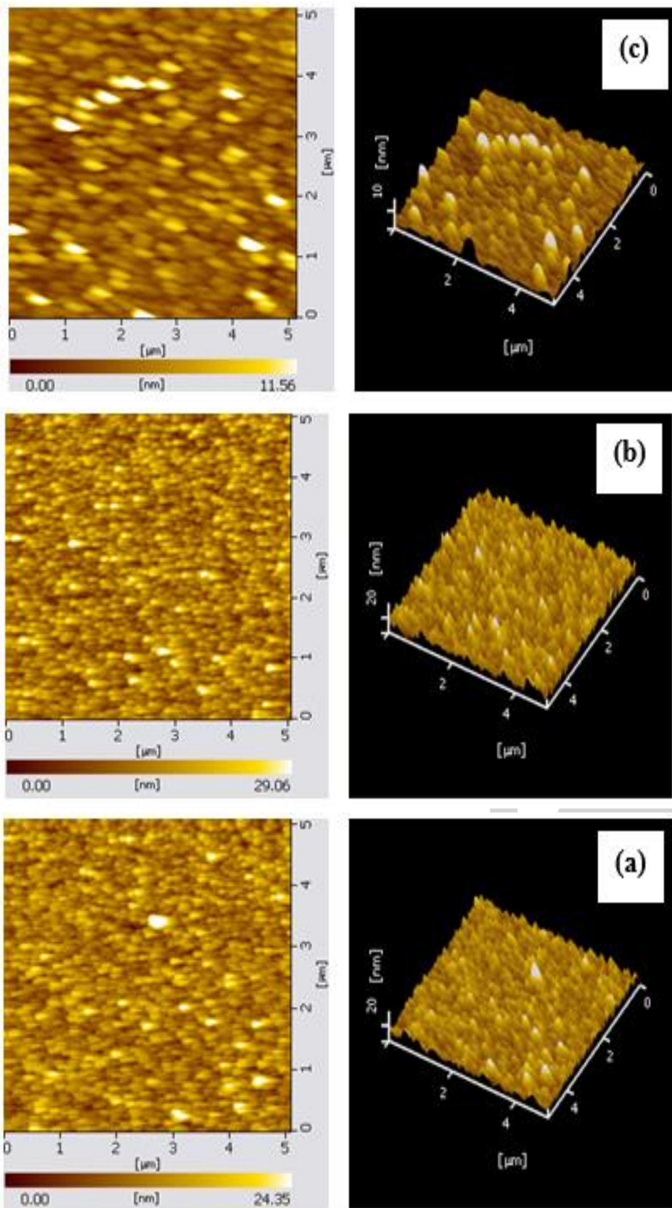

Figure 6 AFM micrographs of nickel oxide films formed at various oxygen partial pressures.

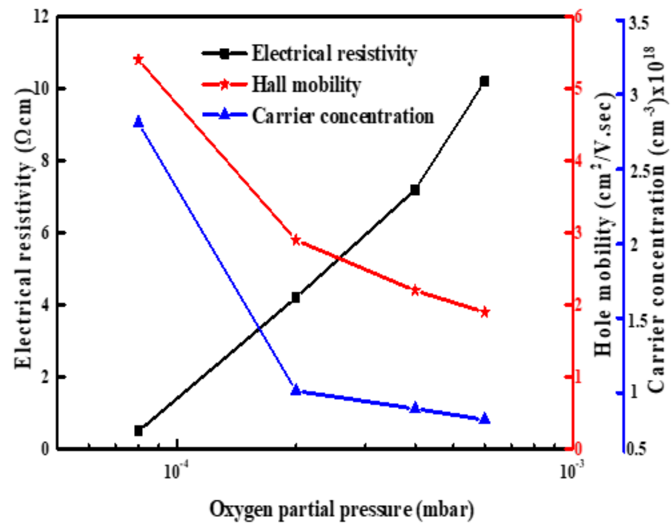

Figure 7 Electrical resistivity of NiO films deposited at various oxygen partial pressures.

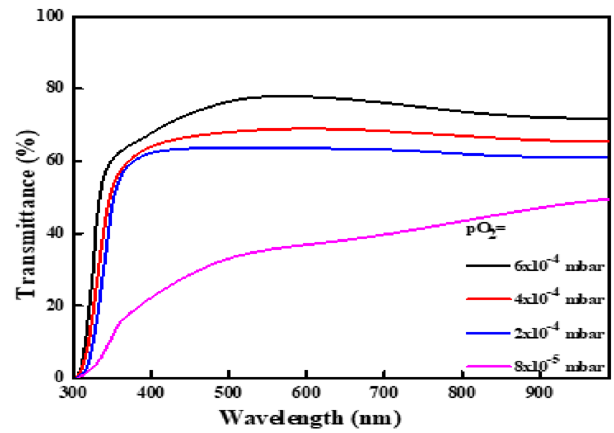

Figure 8 Optical transmittance spectra of NiO films formed at different oxygen partial pressures.

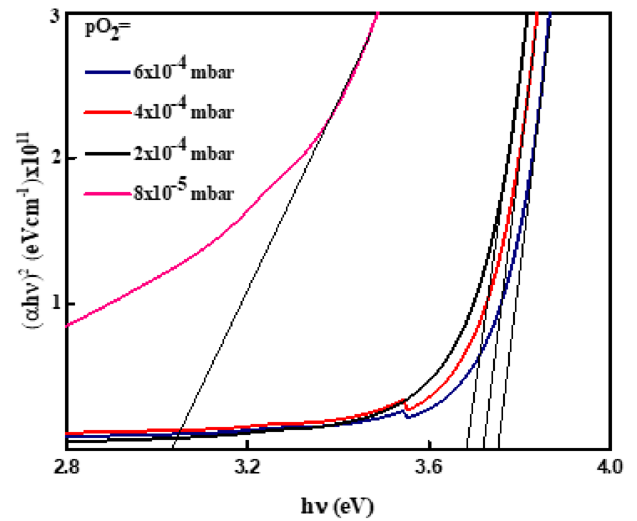

Figure 9 Plots of $(\alpha h\nu)^2$ versus photon energy of NiO films formed at different oxygen partial pressures.

 DOI : 10.35291/2454-9150.2020.0656 © 2020, IJREAM All Rights Reserved.